Metal Ion Assisted Channelling of Substrates in Gold Nanoparticle Catalyzed Reactions

Thesis submitted towards the partial fulfillment of BS-MS Dual Degree Program (2015-2020)

By

Shana Shirin V.

(Reg.No: 20151118)

Under the guidance of

Dr. Pramod P. Pillai

Associate Professor, Department of Chemistry

Indian Institute of Science Education and Research, Pune

Certificate

This is to certify that this dissertation entitled ***'Metal Ion Assisted Channelling of Substrates in Gold Nanoparticle Catalyzed Reactions'*** towards the partial fulfillment of the BS-MS dual degree program at the Indian Institute of Science Education and Research (IISER), Pune represents study/work carried out by **Shana Shirin V.** at **IISER Pune** under the supervision of **Dr. Pramod P. Pillai**, Associate Professor, Department of Chemistry during the academic year 2019-2020.

Signature of Student

Signature of Supervisor

Date: 8 April 2020

Dedicated to

My Family and All Loved Ones

Declaration

I hereby declare that the matter embodied in the report entitled ***'Metal Ion Assisted Channelling of Substrates in Gold Nanoparticle Catalyzed Reactions'*** are the results of the work carried out by me at the Department of Chemistry, Indian Institute of Science Education and Research (IISER), Pune, under the supervision of **Dr. Pramod P. Pillai** and the same has not been submitted elsewhere for any other degree.

Signature of Student

Signature of Supervisor

Date: 8 April 2020

Acknowledgment

Here, I can undoubtedly say that this page holds all the dignitaries of my thesis and gave birth to the rest of the pages comprised in it. Those awesome people who are highlighted here directly or indirectly contributed to this work for its successful fulfillment. I would like to take this opportunity to express my sincere gratitude to each one of them for their valuable assistance, and even their presence in some cases.

Foremost, I wish to convey my deepest gratitude to my supervisor, **Dr. Pramod P. Pillai** (IISER Pune) who introduced me to the *NanoAlchemy research group* and made it a family for me. In addition to his constant suggestions and directions throughout the project, his interaction and support beyond as an advisor were really encouraging and appreciable. Moreover, I wish to thank him for each memorable celebrations we had within and out of the lab.

I would like to pay my special regards to my TAC member**, Dr. Nirmalya Ballav** for his significant suggestions during the course of my project. Also, I would like to thank **Prof. Jayant B. Udgaonkar** (Director, IISER Pune), **Prof. H. N. Gopi** (Chair, Department of Chemistry, IISER Pune) and **Department of Chemistry** for providing a wonderful academic and research facilities to explore.

Next, **Anish Rao** who deserves my heartfelt thanks such that he changed his position from ‘the mentor’ to ‘best friend’ in my life. It is very difficult to express my gratitude to him in a few lines. He is the first person who regularly told me that I am capable of doing research. This motivated me in all my problems and encouraged me throughout my research. I was really inspired by the way he approaches problems, his understandings, presentation skill and moreover the effort he put to give his best. He was there with me in all my ups and downs and helped a lot to tackle my limitations and problems inside and outside the lab. Thanks again my best friend!

NanoAlchemy group is one of the most comfortable places for me where my interest in research emerged. The awesome people (**Soumendu**, **Gayathri**, **Sumit**, **Indra**, **Pradyut**, **Kashyap**, **Sarah**, **Vanshika**, **Jasmine** and **Sreeram**) made my research

life more fun and informative. They taught me different laboratory skills and helped me in my experiments despite the time and work needed for it. I wish to thank you all for making a new family.

I am indebted to all my professors at IISER Pune who contributed profoundly to my academic and research life. Especially, **Dr. Angshuman Nag**, **Dr. Muhammed Musthafa,** and **Dr. Anirban Hazra** were stimulated my thoughts to explore my research in Physical chemistry. I would like to thank **Dr. Boomi Shankar** for providing me a clear picture of single-crystal XRD during the course of my thesis.

I express my sincere gratitude to **Vijaykanth**, **Himan**, **Markose,** and **Ruma** for their helping hands to carry out different characterization techniques in between their busy schedule.

Last but not least is my family and friends. I really thank my family who is my constant support and strength even though they were not around me always. The life at IISER Pune will not complete without my friends who treated me with plenty of memorable moments especially **Abdul Raafik**, **Haritha A.S, Fawas, Neethu, Najma, Anjana, Nazia, Namithasree, Aysha** and **Theja**. I wish to show my hearty thanks to all of them.

Table of Contents

List of Figures

List of Tables

Abstract

In the present thesis, we revisit one of the traditional and benchmark reactions in the area of nanoparticle catalysis, namely the gold nanoparticle (AuNP) catalyzed reduction of para-nitrophenol (PNP) to para-aminophenol (PAP) by sodium borohydride. It has been shown that the ability to govern and dictate the interactions between different reaction components can have prodigious effects on the reaction rates. In this direction, our group has recently shown that regulation of surface potential around a gold nanoparticle (AuNP) catalyst can render the same nanoparticle (NP) system as an efficient catalyst, or as a non-catalyst. It should be noted that most of the studies on AuNP catalyzed PNP reduction can be categorized into two directions:- a) finding the design principles to create best catalysts (like optimizing catalyst shape and crystallinity, ligand hydrophobicity, catalyst-reactant interactions, etc.), and b) finding the best reaction conditions for carrying out efficient catalysis (like the effect of light irradiation, dissolved oxygen, pH, etc.). To the best of our knowledge, all of the studies utilize sodium borohydride as the reducing agent, and relatively little is known about the effect of reducing agents on the PNP reduction reaction. With this in mind, the work presented here aims to find out the optimized reaction conditions (with respect to the reducing agent) for carrying out efficient catalysis. We demonstrate that the strengths of reducing agent (an intuitive parameter) is an incomplete descriptor governing the rate of PNP reduction reaction. Additionally, the metal cations constituting the borohydride salt, can differentially bridge with PNP molecules, thereby increasing the local concentration of reactant molecules around the AuNP catalyst. Thus, our studies reveal that both strength and bridging ability of the reducing agents plays a key role in the PNP reduction. Furthermore, similar trends were observed with AuNPs of different surface chemistries, demonstrating the generality of our findings. The idea of incorporating of bridging interaction between metal ions (from reducing agent) and reactants is powerful enough to convert a non-catalytic system to a catalytically active one. We believe that our study shows how simple variations in the reaction conditions can help in making significant impacts in the field of chemical transformations.

1

Introduction

The '*sea of electrons'* present in metal nanoparticles (NPs) can serve as an electron source for driving a wide-range of oxidation and reduction reactions.[1–10]Decades of research in the field of nanocatalysis have helped in introducing different metal NP based catalysts for many chemical tranformations.[1–10]Chief among them is borohydride (BH_4^-) mediated reduction of para-nitrophenol (PNP) to para-aminophenol (PAP).[3,11–13]This reaction has been so widely studied that it has become a model reaction for testing the catalytic efficiencies of various NPs.[7,10,13–20]Here, borohydride mediated reduction of PNP, *despite being thermodynamically feasible*, proceeds only in the presence of a suitable catalyst. During the course of reaction, the surface of NPs act as the adsorption sites for reactant molecule (PNP) and borohydride ions, thereby facilitating the transfer of an electron between the two moieties.[21,22]This passive participation of NPs helps to overcome the kinetic barrier associated with the reaction, resulting in an efficient reduction of PNP molecules.[21,22]Several studies have been undertaken to identify the optimized factors and conditions, capable of carrying out efficient catalysis. In this direction the studies that have been undertaken can be categorized into two directions:-

a) optimizing the design principles to create best catalysts (like catalyst shape and crystallinity, ligand hydrophobicity, ligand packing, catalyst-reactant interactions, etc.)[21,23–30], and

b) optimizing the best reaction conditions for carrying out efficient catalysis (like the effect of light irradiation, dissolved oxygen, pH, etc.).[23,31–33]

Most of the studies in literature have focused on studying the role, and effect of NP's crystallinity, hydrophobicity of ligands, surface area of the catalyst, etc. on PNP reduction.[21,23–30]These understandings have helped in establishing design principles for making new generation of efficient catalysts. Recently, some studies have been undertaken to understand the effects of different environmental conditions on the

PNP reduction reaction. Notable among them is the role of light irradiation in facilitating the reduction reaction, and the role of dissolved oxygen in affecting the catalysis.[23,31–33]Surprisingly, all of the studies utilize sodium borohydride as the reducing agent, and relatively little is known about the effect of reducing agents on the PNP reduction reaction. This is possibly because of the intuitive chemical understanding that a reduction reaction relies on the reducing power of reductant.[34,35]So modifying the reductant to a stronger one should, intuitively, improve the rate of reduction reaction. A conclusive and thorough investigation in this direction is presented here, where, we study the effect of strengths of the reducing agent on PNP reduction reaction. It is well known that the strength of borohydride reducing agent is dictated by the lewis acidity of the metal ions in the salt.[34,35]With this in mind, we performed systematic studies by adding different metal salts to the reaction mixture for the in-situ production of stronger borohydrides, in accordance with established literature protocols.[36]

The present work shows the prodigious, and counterintuitive effects of metal ions (comprising the borohydride salt) on the AuNP catalyzed PNP reduction reaction. For this, AuNPs functionalized with N,N,N-trimethyl(11-mercaptoundecyl)ammonium chloride (TMA, [+]) were used to efficiently catalyze the reduction of PNP molecule.[11]It was observed that the addition of different metal cations (like Ca^{2+}, Mg^{2+}, Li^{+}) could accelerate the rate of PNP reduction. A common understanding of chemistry would attribute these accelerated reaction rates to the strength of reducing agents used. In the present study, we show that strengths of the reducing agent is an incomplete descriptor, and one needs to take into account *specific-ion effects* to completely explain the observed trends in the rate of PNP reduction. More specifically, metal cations can not only influence (*speed up*) the reaction by increasing the reducing power of borohydride, but also bridge with the PNP molecule and help in the efficient reduction process. Both these combined effects were then used to convert non-catalytic amounts of AuNPs to catalytic systems, which helped in reducing the amount of catalyst to ~5 pM (0.03 mol %). We observed similar increments in the reaction rates upon the addition of different metal ions with AuNPs having different surface chemistries as well. We believe that our study shows how simple variations in the reaction conditions can help in making significant impacts in the field of chemical transformations.

2

Materials & Methods

2.1. Materials and Reagents

Tetrachloroaurate trihydrate ($HAuCl_4.3H_2O$), Tetramethylammonium hydroxide (TMAOH) 25 % wt. in water, 11-mercaptoundecanoic acid (MUA), Hydrazine monohydrate ($N_2H_4.H_2O$ 50-60%), Tetrabutylammonium borohydride (TBAB), p-Nitrophenol (PNP), Nitrobenzene (NB), divalent and monovalent salts:- Calcium chloride dihydrate ($CaCl_2.2H_2O$), Lithium chloride (LiCl), Magnesium chloride hexahydrate ($MgCl_2.6H_2O$), Potassium chloride (KCl), and Sodium chloride (NaCl) were purchased from Sigma Aldrich. (Di-n-dodecyl)dimethyl ammonium bromide (DDAB) and Dodecylamine (DDA), were purchased from Alfa Aesar. All experiments were carried out without further purification of supplied reagents. All the stock solutions of metal ions were prepared in milliQ water (Resistivity = 18.2 MΩ.cm at 25^0C). N,N,N-trimethyl(11-mercaptoundecyl)ammonium ion (TMA – positively charged) was synthesized according to the reported procedure.[37]

2.2. Synthesis of [+], [-] and $[+/-]_4$ AuNPs: Place Exchange Method

2.2a) Synthesis of DDA-Capped AuNPs

All the nanoparticles were synthesized via place exchange reaction of DDA-Capped AuNPs (DDA-AuNPs). DDA-AuNPs in toluene were prepared firstly according to a modified literature report.[11,38–40]$HAuCl_4.3H_2O$ was used as the gold precursor, and a mixture of hydrazine monohydrate and TBAB was used as the reducing agent in the modified procedure. Solution A was prepared using $HAuCl_4.3H_2O$ (~15 mg, 1 eq.), DDA (~135 mg, 20 eq.), and DDAB (~148 mg, 10 eq.) in 4 mL toluene. Similarly, Solution B was prepared by mixing TBAB (~36 mg, 3.8 eq.) and DDAB (~60 mg, 4 eq.) in toluene (~1.7 mL). Both the solutions A, and B were sonicated for ~15 mins to completely solubilize the reagents. Solution B was rapidly injected to Solution A along with stirring, which resulted in an immediate color change from yellow to brown

(Seed solution). The as prepared seeds were then aged overnight. Next, seed particles were grown to 5.6 ± 0.9 nm using growth solution which was prepared by mixing $HAuCl_4.3H_2O$ (~143 mg, 10 eq.), DDA (~1.7 g, 250 eq.) and DDAB (~592 mg, 40 eq.) in ~36 mL toluene with seed solution along with stirring. The resulting solution was further reduced by the dropwise addition (in ~30 min) of solution (~15 mL) made up of hydrazine monohydrate (~183 µL, 80 eq.) and DDAB (minimum amount required for a clear transparent solution) in toluene. The solution was left for stirring overnight resulted in the formation of monodisperse DDA-AuNPs of size 5.6 ± 0.9 nm.

2.2b) Place Exchange Reaction

DDA-AuNPs were equally divided into 3 conical flasks to synthesize [+], [-],and $[+/-]_4$ AuNPs respectively. Each set of DDA-AuNPs were purified using methanol (50 mL) resulting in the precipitation of DDA-AuNPs which was redispersed in toluene (20 mL) after decanting the supernatant. In the place exchange reaction, solution of [+] and [-] ligands in 10 mL of dichloromethane (DCM) was added to purified DDA-AuNPs and kept overnight for complete place exchange. Next, the precipitates were collected by discarding the supernatant and washed with DCM (3 x 50 mL), and finally with acetone (50 mL), dried, and redispersed in deionized water with the addition of 20 µL of TMAOH. In the case of $[+/-]_4$ AuNPs, place exchange was carried out in the presence of both [+] and [-] ligands in the ratio of 1:4.

2.3. Characterization Techniques

2.3a) Zeta Potential (ζ) Studies

Zeta potential of all the charged AuNP solutions (pH ~7) were performed using Nano ZS90 (Malvern) Zetasizer instrument. In all measurements, the optical density of NP solutions kept around ~0.3. ζ was obtained by measuring the electrophoretic mobility of AuNPs and using Henry's equation.

Henry's equation is

$$U_E = \frac{2\varepsilon z f(\kappa_a)}{3\eta}$$

Where,

U_E = Electrophoretic mobility

Z = Zeta potential

Ɛ = Dielectric constant

η = Viscosity

$f(K_a)$= Henry's function

Smoluchowski's approximation was used to measure the zeta potential values of NPs. The ζ values reported are based on an average of 5 measurements.

2.3b) Transmission Electron Microscopic (TEM) Studies

The High-resolution Transmission Electron Microscopic (HRTEM) studies were performed on TECNAI G2 20 TWIN at 200 kV. Diluted solutions of AuNPs were drop-casted on 400 mesh carbon-coated copper grids (Ted Pella Inc.) and removed solvents carefully using tissue paper after keeping the sample undisturbed for ~10 mins. This method minimizes the appearances of artifacts due to drying effect. Imaging was carried out after the complete drying of samples under vacuum.

2.4. Catalytic Reduction

Kinetics of all AuNP mediated reduction reactions were monitored using UV-Vis absorption spectroscopy (SHIMADZU UV-3600 plus UV-VIS-NIR spectrophotometer). The reaction mixture was prepared in 3 mL cuvette (path length = 1 cm), and the absorption spectra were collected with a time interval of 5 min up to a maximum of 2 h, unless stated otherwise. The time-dependent kinetic experiments were performed by recording the absorbance of the reactant at its λ_{max} with time. All tests were performed under room temperature except the temperature-dependent kinetic studies. UV-Vis spectrophotometer connected with an external temperature controller was used for the temperature-dependent studies so as to maintain appropriate temperatures of interest. The concentration of AuNPs was calculated in terms of nanoparticles using 5.4 x 10^7 $M^{-1}cm^{-1}$ as the extinction coefficient[41], and mol % are expressed in terms of Au atoms.

2.4a) Reduction of p-Nitrophenol (PNP)

In a typical AuNP mediated catalytic reduction of p-nitrophenol (PNP) by BH_4^- ions, 300 µL of 0.1 M $NaBH_4$, 15 µL of AuNP solution (1nM, 4nM, etc. according to the desired concentration of NPs in the reaction mixture) and 6 µL of 50 mM PNP and milliQ water was mixed in a cuvette. The total volume of the reaction mixture was maintained as 3 mL. The time-dependent experiment was performed using UV-Vis. absorption spectroscopy by monitoring absorbance at 400 nm with a constant time interval. Catalytic reduction of PNP in the presence of various metal ions and its time-dependent study were performed in a similar fashion, where, we added appropriate concentrations of the metal salt to the solution, after the addition of $NaBH_4$.

2.4b) Reduction of Nitrobenzene (NB)

AuNP mediated NB reduction by BH_4^- ions was performed by mixing 300 µL of 0.1 M $NaBH_4$, 15 µL of 4 nM AuNP solution, 6 µL of 50 mM NB (in MeOH) and milliQ water in a quartz cuvette (total reaction mixture = 3 mL). Absorbance at 279 nm was recorded in a constant time interval. Catalytic reduction of NB in the presence of calcium and magnesium ions and its time-dependent study was performed in the same way where we added metal salt to the solution, after the addition of $NaBH_4$.

2.5. Determination of Conversion, Reaction rate (k') and Rate Constant (k)

The rate of catalytic reduction reaction was determined by assuming the conversion of reactant to the product was first-order in the concentration of PNP. In the case of PNP reduction reaction, the decrease in the concentration (conversion at time t) of p-nitrophenolate at 400 nm was calculated using Beer's Lambert law where 18300 $M^{-1}cm^{-1}$ was used as the molar extinction coefficient of p-nitrophenolate.[42] i.e.,

$$\text{Conversion (t)} = -\frac{\left(A_{400\,nm}(t) - A_{400\,nm}(t=0)\right)}{18300}$$

In the case of NB reduction reaction, the conversion of NB to aniline proceeded through an intermediate which is N-phenylhydroxylamine.[43,44] The reaction rate was determined based on the conversion of N-phenylhydroxylamine to aniline at its λ_{max} where 1000 $M^{-1}cm^{-1}$ used as the molar extinction coefficient of N-phenylhydroxylamine at 279 nm.[45] i.e.,

$$\text{Conversion (t)} = -\frac{\left(A_{279\,nm}(t) - A_{279\,nm}(t=0)\right)}{1000}$$

The reaction rate was determined by fitting the conversion vs. time (*t*) plot with a function given below

$$c = c_0\,(1 - e^{-kt})$$

Here, c_0 stands for initial concentration of PNP and N-phenylhydroxylamine in PNP and NB reduction reaction respectively and k stands for the rate constant of the reaction. Rate of reaction is represented below

$$\frac{dc}{dt} = c_0.k.e^{-kt}$$

Reaction rate at t = 0 is given as

$$k' = \frac{dc}{dt}(t=0) = c_0.k$$

The rate constant, k was determined by the following equation

$$k = \frac{k'}{c_0}$$

Where c_0 was taken as 10^{-4} M in the case of PNP and corresponding initial concentration of N-phenylhydroxylamine in NB reduction with the presence and absence of metal ions.

2.6. Crystallographic Study

2.6a) Preparation of Crystals

All crystals used for the studies were prepared by a method of slow evaporation of the solvent at room temperature. Firstly, calcium hydroxide and magnesium hydroxide were prepared by adding $CaCl_2.2H_2O$ and $MgCl_2.6H_2O$ with NaOH in milliQ water resulted in the formation of white precipitates of respective hydroxides. Further, precipitates were collected by centrifugation and washed with milliQ water. These precipitates dried completely after decantation of the supernatant. Crystals of PNP with $Ca(OH)_2$ were produced by slow evaporation of solvent from the bright transparent yellow colored solution which contained 50 mM PNP and 25 mM

$Ca(OH)_2$ in milliQ water. Similarly, crystals of PNP with $Mg(OH)_2$ prepared and orangish yellow crystals were formed in both cases within 2 weeks.

2.6b) Single Crystal X-ray Diffraction

Single-crystal X-ray diffraction studies for all the p-nitrophenolate salts were performed by collecting reflections on a Bruker Smart Apex Duo diffractometer using Mo Kα radiation (λ = 0.71073 Å). The structures were refined by using the full-matrix least-squares method against F^2 using all data by SHELXL-2017 built in the Apex 3 suite. Crystallographic refinement data for all of the salts are listed in the following **Table 2.6.1.** All of the non-hydrogen atoms were refined anisotropically if not stated otherwise. Hydrogen atoms were constructed in geometric positions to their parent atoms.

Compound	**Calcium-paranitrophenolate**	**Magnesium-paranitrophenolate**
Chemical system	Monoclinic	Monoclinic
Space group	P 1 21/n 1	P 1 21/c 1 (14)
a	13.1605(12) Å	12.3698(15) Å
b	3.6268(3) Å	6.6167(8) Å
c	16.9855(15) Å	11.7758(14) Å
α (°)	90°	90°
β (°)	90°	90°
γ (°)	93.414(5)°	93.553(3)°
Cell Volume	**809.29(12) Å^3**	**961.96(20) Å^3**

Table 2.6.1. Crystallographic data for calcium and magnesium 4-nitrophenolate salts.

3

Results & Discussion

In order to study the effect of reaction conditions on nanocatalysis, we selected the model catalytic reaction of PNP reduction by sodium borohydride ($NaBH_4$) in the presence of AuNP. The reaction depends on the adsorption of substrates (BH_4^- and PNP) on the surface of AuNPs which helps in overcoming the kinetic barrier of the reaction. In this direction, we build on the work developed in our group, where interactions emanating from the surface ligands could render the same AuNP as an efficient catalyst or a non-catalyst.[11]With this in mind, we worked with positively charged AuNPs ([+] AuNPs) which could direct the substrates ([-] PNP and BH_4^-) towards the AuNP surface, through electrostatic attractions.[11]

3.1. Synthesis of [+] AuNPs

A place exchange protocol was adopted to synthesize [+] AuNPs. For this, we synthesized DDA capped AuNPs having a core diameter of 5.6 ± 0.9 nm, using a modified literature protocol. [11,38-40]DDA ligands on AuNPs were place exchanged with N,N,N-trimethyl(11-mercaptoundecyl)ammonium chloride (TMA [+]) to synthesize [+] AuNPs (**Scheme 3.1.**), see **Section 2.2.** of Materials and Methods for more details.[39,40]

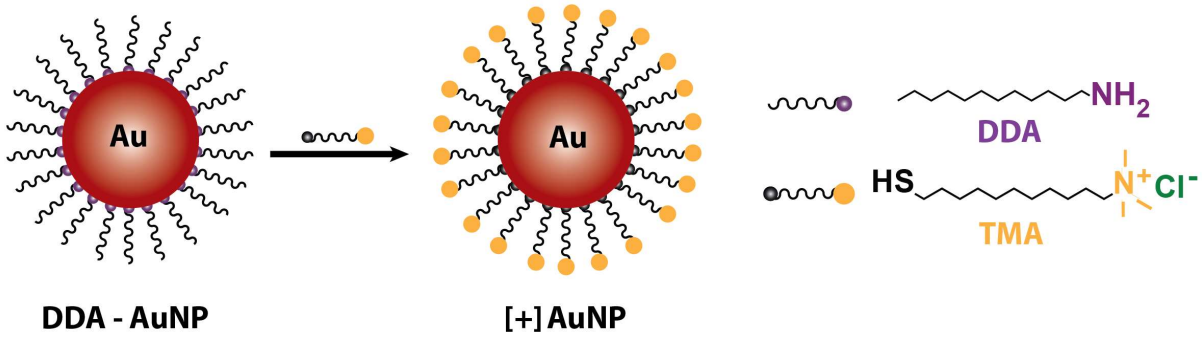

Scheme 3.1. Schematics showing the synthesis of [+] AuNPs through place exchange of DDA-AuNPs.

The synthesized [+] AuNPs were well characterized by UV-Vis. absorption, zeta potential, and transmission electron microscope (TEM) studies (**Figure 3.1.**). We observed a characteristic surface plasmon resonance (SPR) peak at ~520 nm, corresponding to the wine-red color of [+] AuNPs (see **Figure 3.1a**). The average size of the prepared [+] AuNPs was estimated to be 5.6 ± 0.9 nm (see **Figure 3.1c**). A zeta potential value of +38.5 ± 3.2 mV confirms the presence of positive charges on the surface of AuNPs (**Figure 3.1b**). With desired [+] AuNPs in our hands, we used them to catalyze the reduction of p-nitrophenol (PNP) by sodium borohydride ($NaBH_4$), to study the dependence of reduction rate on reaction conditions.

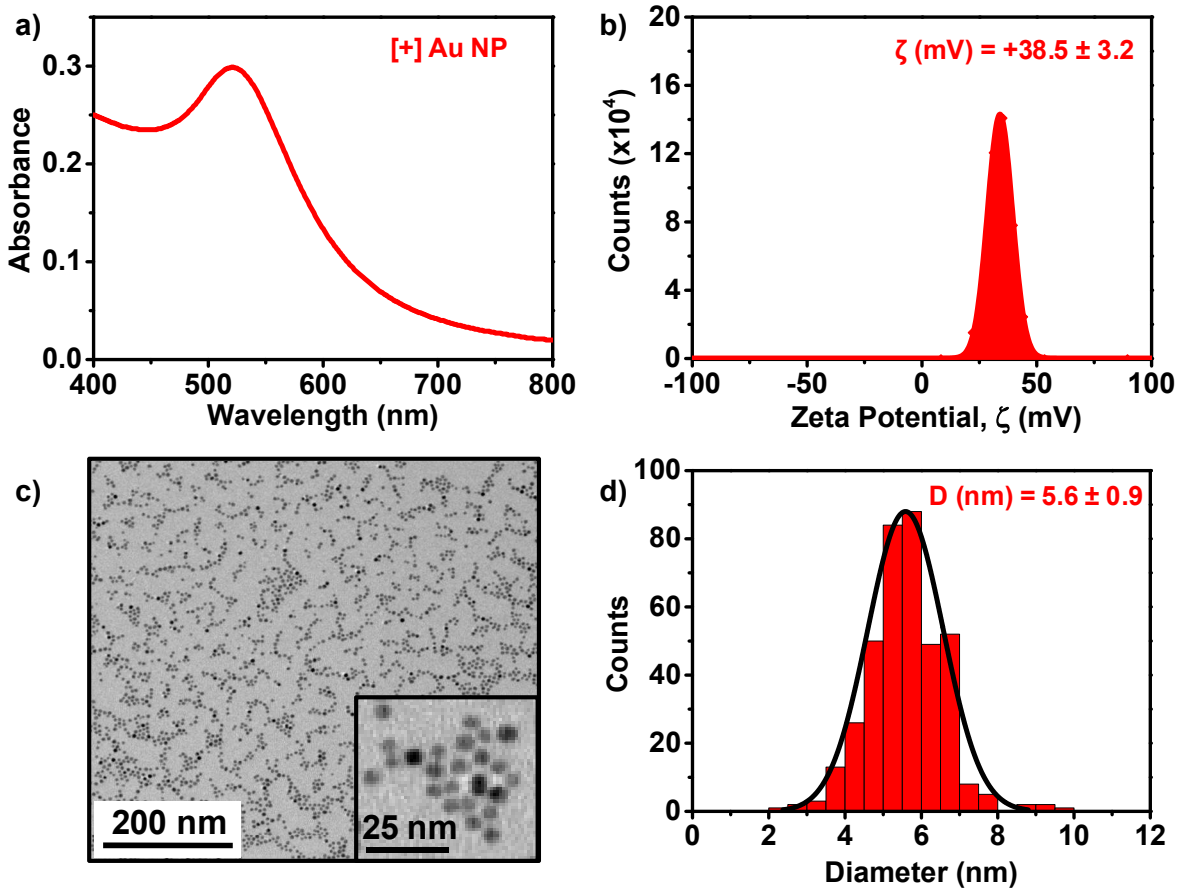

Figure 3.1. Characterization of [+] AuNPs: a) UV-Vis. absorption, b) Zeta potential study, c) Representative TEM image, and d) Size distribution histogram for [+] AuNPs. The average size of [+] AuNPs was estimated by analysing ~300 NPs.

3.2. Catalytic Reduction of PNP

We used 20 pM of [+] AuNPs (0.1 mol % in terms of Au atoms) to catalyze the reduction of PNP (100 μM) to p-aminophenol (PAP) in the presence of an excess

amount of $NaBH_4$ (10 mM). It has been shown that [+] AuNPs can channelize the negatively charged reactant, as well as borohydride to the AuNP surface (in accordance with Langmuir-Hinshelwood mechanism), resulting in efficient catalysis. The progress of the reaction was monitored by following the changes in the UV-Vis. absorption of p-nitrophenolate (at 400 nm) for ~2 h. We observed that [+] AuNPs could swiftly catalyze the reduction in the peak intensity of PNP, along with an associated color change from yellow to colorless (see inset of **Figure 3.2b**). The steady decrease in the absorbance of PNP at 400 nm was associated with a simultaneous appearance of the absorption peak at 300 nm, corresponding to the absorption of p-aminophenolate ion (PAP, **Figure 3.2a**).[3,11–13]Because of the presence of excess amounts of BH_4^- over PNP, the reaction kinetics follows pseudo-first-order kinetics, and the rate constant of the reaction (k) was estimated to be ~0.04 min^{-1} from conversion vs. time plot (**Figure 3.2b**) (see **Section 2.5**. for more details).

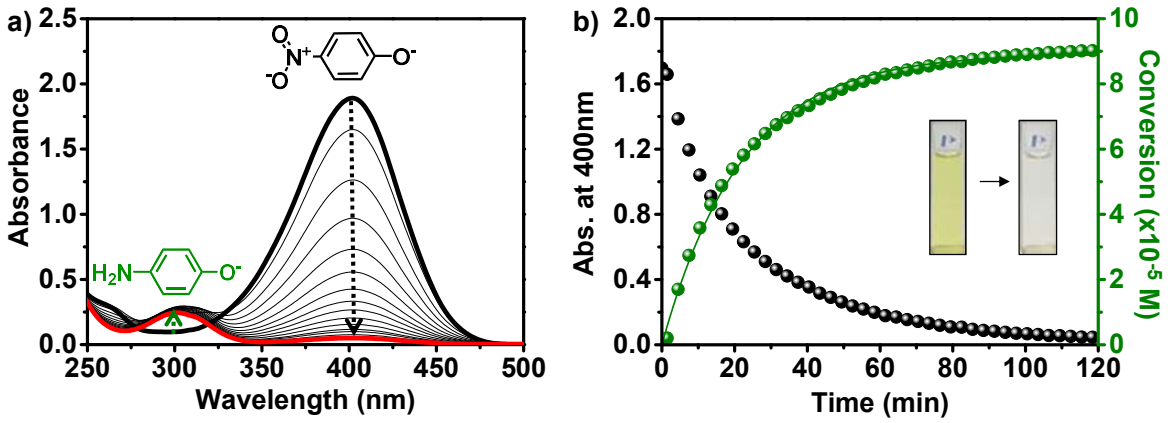

Figure 3.2. [+] AuNP catalyzed reduction of PNP by $NaBH_4$: a) Gradual decrease in the absorbance of PNP (at ~400 nm; shown with black arrow), along with a concomitant increase in the absorption of PAP (at 300 nm; shown with green arrow) in the presence of 0.1 mol % [+] AuNPs, and b) Progress of the reaction, along with the conversion (shown in green) for the first-order kinetic fitting. Inset shows the visible color change before and after the reduction of PNP.

Various studies documented in the literature have provided a detailed understanding of design principles enabling the development of efficient catalysts. However, studies investigating the role of reaction conditions on the catalytic activities of NP systems are barely investigated in the literature, even though they are equally significant factor for efficient catalysis. Towards this, the present work

aims to investigate the effect of reducing agents on AuNP catalyzed reduction of PNP by BH_4^- ions.

In the present reaction, sodium borohydride ($NaBH_4$) acts as the reducing agent, and it may be intuitive to understand that stronger borohydrides (reducing agents), will increase the reaction rate. More precisely, the use of stronger reducing agents like lithium borohydride ($LiBH_4$), calcium borohydride ($Ca(BH_4)_2$), magnesium borohydride ($Mg(BH_4)_2$), etc. can improve the rate of PNP reduction.[34–36]Furthermore, different metal borohydrides can be prepared in-situ by the addition of metal ions to $NaBH_4$.[36]With this in mind, we envisaged that the addition of metal ions in our reaction mixture can enhance the reaction rate by increasing the strength of metal borohydrides. In this direction, first, we started with the addition of 10 mM Ca^{2+} ions (equal to the amount of BH_4^- in the reaction) to test our hypothesis.

3.3. Effect of Calcium Ions in Catalytic Reduction of PNP

The catalytic reduction of PNP in the presence of Ca^{2+} ions (10 mM) was carried out under similar reaction conditions, as were used in **section 3.2.** In a typical reaction, 10 mM Ca^{2+} was added to a 10 mM solution of $NaBH_4$, followed by the addition of 20 pM of [+] AuNPs and 100 µM PNP. The reaction was then monitored by UV-Vis. absorption spectroscopy at room temperature for ~2 h. The addition of Ca^{2+} ions to the reaction mixture resulted in dramatic acceleration (~12 times improvement) in the reduction rate of PNP, compared to the reduction in the absence of Ca^{2+} ions. The reaction completed in ~15 min, as opposed to ~2 h in the absence of Ca^{2+} (see **Figure 3.3.1a**). **Figure 3.3.1b** shows the first-order kinetics of the reaction in the presence (red curve) and absence (green curve) of Ca^{2+} ions, and the corresponding rate constant values are given in the inset. Control experiments performed in the absence of [+] AuNPs showed no reduction of PNP even after ~2 h, showing the inability of $Ca(BH_4)_2$ (a stronger reducing agent) alone to reduce PNP (see blue spectrum in **Figure 3.3.1b**). This confirms the necessity of [+] AuNPs to catalyze the conversion of PNP to PAP even in the presence of stronger reducing agents like $Ca(BH_4)_2$.

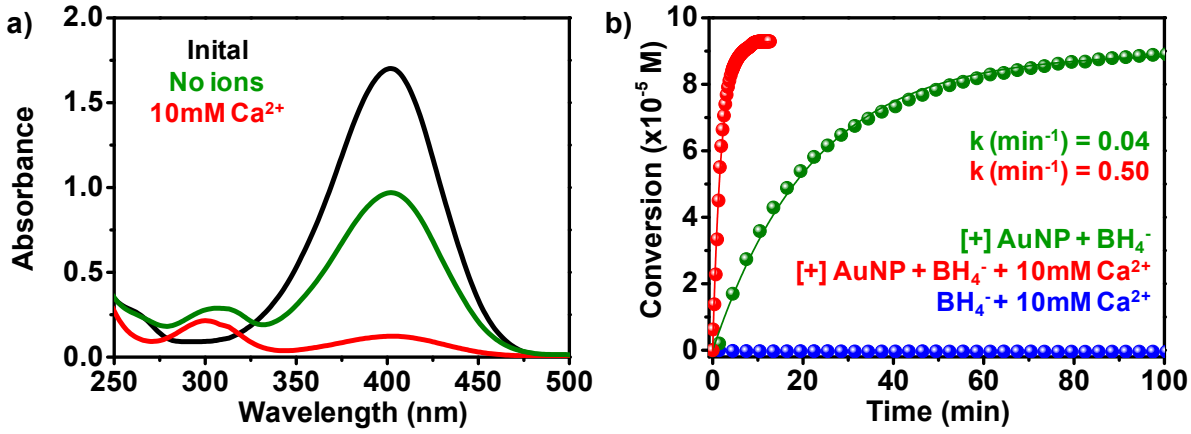

Figure 3.3.1. Effect of Ca^{2+} ions on [+] AuNP catalyzed reduction of PNP by BH_4^- ions: a) Absorption changes during the [+] AuNP (0.1 mol %) catalyzed reduction of PNP by BH_4^-, after 15 min, in the presence (red) and absence (green) of Ca^{2+} ions, and b)the corresponding first-order kinetic fit (red and green). Blue data represents negligible reduction of PNP in the absence of AuNPs even in the presence of 10 mM Ca^{2+} ions.

The PNP reduction reaction proceeds in accordance with Langmuir-Hinshelwood mechanism.[11,21]According to this mechanism, AuNPs help in overcoming the kinetic barrier of the reaction by acting as adsorption sites for both PNP and borohydride molecules, and mediate the transfer of electrons between the two. Furthermore, the effect of Ca^{2+} ions on the activation energy of PNP reduction by 20 pM of [+] AuNPs was investigated by monitoring the reaction rates in the absence (**Figure 3.3.2a**) and presence (**Figure 3.3.2b**) of Ca^{2+} ions at different temperatures. The activation energies were estimated from the slope of a linear fitting between ln(k) vs. 1/T graphs. Interestingly, we observed an appreciable decrease in the apparent activation energy for PNP reduction by BH_4^-, from ~52 kJ/mol (in absence of Ca^{2+}) to ~16 kJ/mol (in presence of Ca^{2+}), see **Figure 3.3.2.** Next, our focus was to ascertain whether the addition of other metal ions will result in similar improvements in the reaction rates.

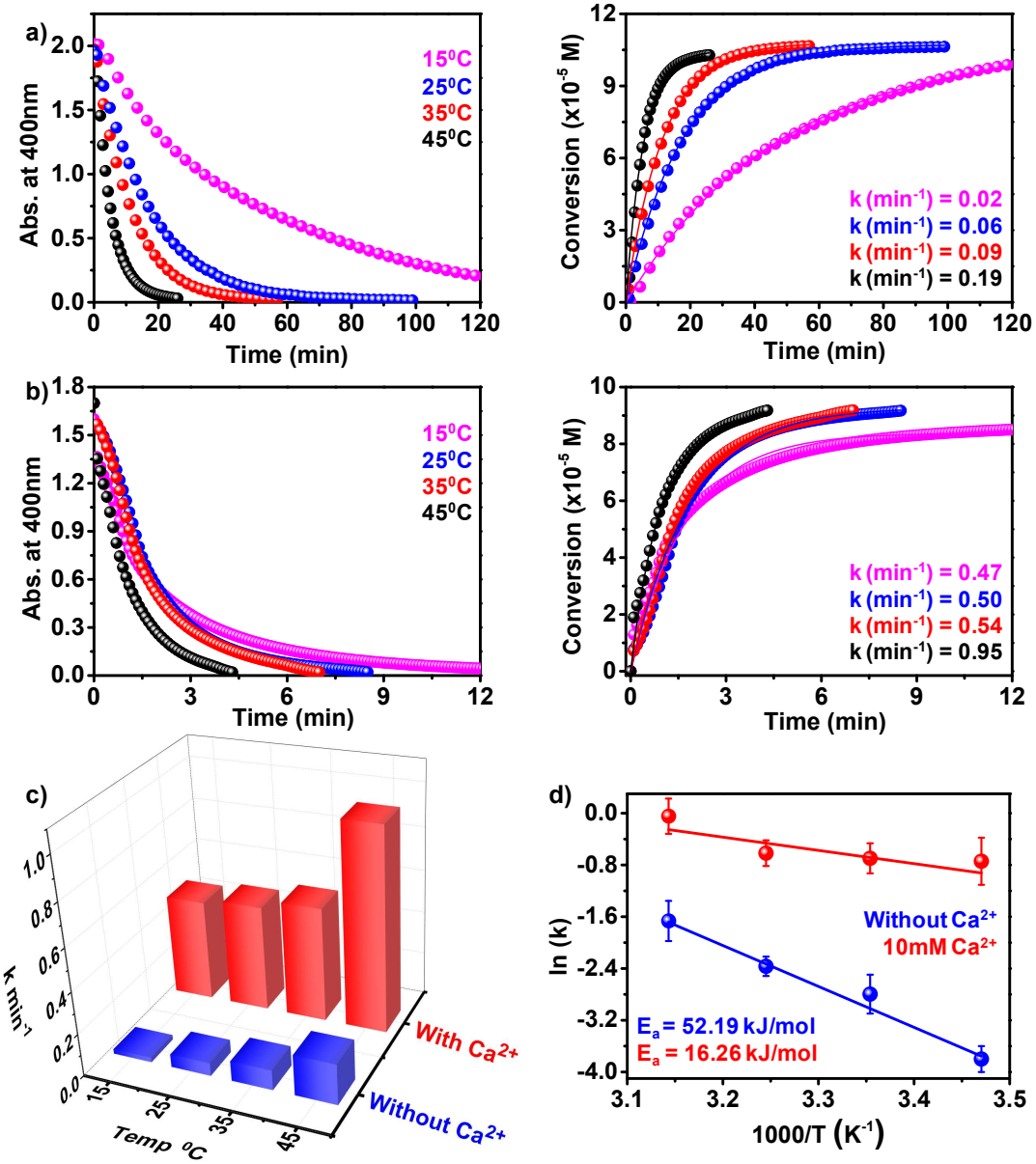

Figure 3.3.2. Temperature-dependent experiments to estimate activation energies: UV-Vis. absorption changes at 400 nm and their corresponding first-order rate fittings at different temperatures in the a) absence, and b) presence of 10 mM Ca^{2+} ions, c) Plot showing the variation in the rate constant of PNP reduction with temperature, and d) Plot of ln(k) vs. 1000/T to estimate the activation energies in the presence, and absence of Ca^{2+} ions. All experiment were carried out with 0.1 mol % of [+] AuNPs.

3.4. Metal Ions Dependent Catalytic Reduction of PNP

We performed a series of reactions, to understand the influence of different metal ions on [+] AuNP catalyzed PNP reduction by BH_4^- ions. In a typical experiment, 10 mM Mg^{2+} was added to a 10 mM solution of $NaBH_4$, followed by the addition of 20

pM of [+] AuNPs and 100 μM PNP (for more details on experimental conditions, see **Section 2.4a**). The reaction was then monitored by UV-Vis. absorption spectroscopy at room temperature for ~2 h (blue spectrum in **Figure 3.4.**). Here again, we observed a dramatic increase in the reaction rate from 0.06 min^{-1} to 0.29 min^{-1} (~5 times improvement in reaction rate), compared to the reduction in the absence of Mg^{2+} ions. Similar experiments were performed with other metal ions like K^+, Li^+, and Na^+ as well. Note: we could not perform experiments with other divalent metal ions like Zn^{2+}, Mn^{2+}, Co^{2+}, etc. and trivalent metal ions like Al^{3+}, Fe^{3+}, because of their unsuitability under basic reaction conditions (the divalent ions resulted in the formation of insoluble hydroxides, and Al^{3+}, being acidic in nature, resulted in a pH drift to neutral/ acidic pH values).

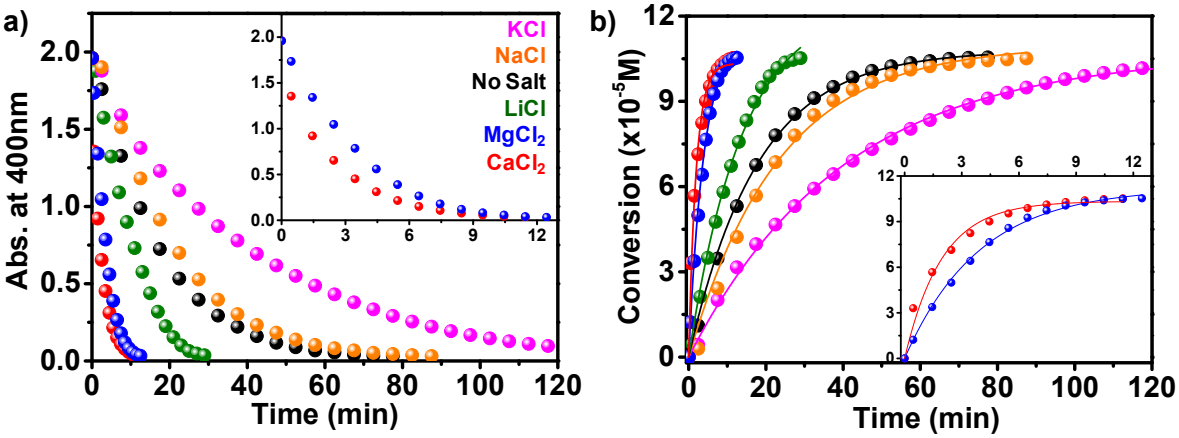

Figure 3.4. [+] AuNP catalyzed reduction of PNP by BH_4^- with monovalent and divalent ions: a) UV-Vis. absorbance changes in characteristic peak of PNP (at 400 nm) during 0.1 mol % [+] AuNP catalyzed reduction of PNP by BH_4^- in the presence of different metal ions (10 mM), and b) corresponding conversion graphs for the first-order kinetic analysis. The reduction rates depend on the presence of metal ions in the following order: K^+< Na^+< Li^+< Mg^{2+}< Ca^{2+}.

After performing PNP reductions in the presence of different cations (K^+, Na^+, Li^+, Mg^{2+}, Ca^{2+}), the reaction rates can be arranged in the following order: K^+< Na^+< Li^+< Mg^{2+}< Ca^{2+} (see **Figure 3.4, Table 3.4.1.**). Some key points to be noted from the observed experimental trends in **Figure 3.4,** and **Table 3.4.1.** are summarized below:-

a) Divalent ions showed accelerated reaction rates when compared with monovalent ions. This is possibly due to stronger lewis acidity of divalent ions over monovalent ions, resulting in the formation of stronger reducing agents.[34-36]

b) For monovalent ions, we observe that Li^+ being a stronger lewis acid, can accelerate the reaction rate (green curve in **Figure 3.4.**) over Na^+, while K^+ (pink curve in **Figure 3.4.**) retards the reaction rate because of it weaker lewis acidity when compared to Na^+.

c) For divalent ions, surprisingly, we observed that Ca^{2+} (red curve in **Figure 3.4.**), despite being a weaker lewis acid than Mg^{2+} (blue curve in **Figure 3.4.**), shows ~2 times accelerated reaction rates than Mg^{2+}.

These results demonstrate the strengths of the metal borohydride, or lewis acidity of the metal ion, is an incomplete/ partial descriptor for the variations observed in reaction rate trends.

S.No.	Metal Salt (10 mM)	Lewis Acidic Strength of Cation[46]	k (min^{-1})
1	KCl	0.13	0.03
2	NaCl	0.16	0.05
3	No Salt	0.16	0.06
4	LiCl	0.21	0.09
5	$MgCl_2$	0.33	0.29
6	$CaCl_2$	0.27	0.53

Table 3.4.1. Rate constant of [+] AuNP catalyzed reduction of PNP by BH_4^- in the presence of various metal salts and their lewis acidic strength.

This counterintuitive observation of weaker reducing agent ($Ca(BH_4)_2$) being better for PNP reduction than $Mg(BH_4)_2$ (a stronger reducing agent), indicates the involvement of some other factors in the PNP reduction reaction. We hypothesized the existence of *specific-ion* effects like differences in coordination abilities with PNP can also affect the reaction rate. Where, if the metal ions could bridge with PNP, it will result in improved substrate channelling and local concentration, thereby accelerating the reaction rate (see **Scheme 3.4.**). We, therefore, hypothesized that combined effects of reducing abilities, as well as *specific-ion* effects like coordinating ability of metal ions, are better and complete descriptors for explaining the observed variations in the reaction rates.

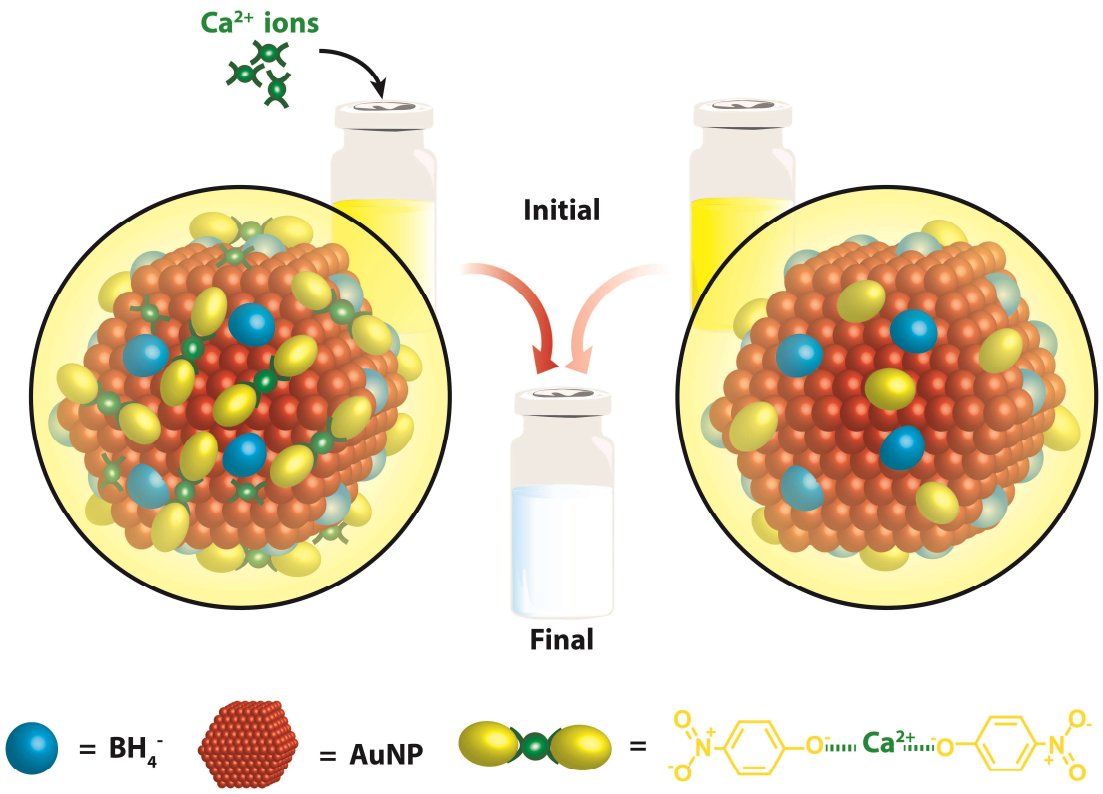

Scheme 3.4. Schematic representation showing the effect of coordination abilities of calcium (left) with PNP in channelling and increasing the local concentration of reactant molecules around AuNP catalyst, thereby accelerating the PNP reduction.

With this in mind, we performed two systematic, and independent experiments to validate our hypothesis of *specific-ion* effects (bridging/coordination) influencing the PNP reduction reaction. First, we used single-crystal XRD studies to study how Ca^{2+}, and Mg^{2+}, interacts with PNP molecules. Second, we performed the [+] AuNP mediated catalytic reduction of nitrobenzene (NB) by BH_4^- ions, where there is no possibility of bridging through the alcohol group.

3.5. Crystallographic Study of PNP with Metal Ions

In order to visualize the *specific-ion* effects (like bridging between metal ions, and PNP molecule) in influencing the rate of PNP reduction, we crystallized Ca^{2+} and Mg^{2+} 4-nitrophenolate salts. For a detailed description of the crystallization protocol, see **Section 2.6**. Here, we observe that calcium 4-nitrophenolate (**Figure 3.5a**) crystallizes with Ca^{2+} ions interacting with 6 oxygen atoms: 2 from water, and 4 from the hydroxyl group in the 4-nitrophenolate molecule, indicating coordination between Ca^{2+} and 4-nitrophenolate. On the other hand, Mg^{2+} crystallizes by interacting with 6

oxygen atoms, all belonging to water molecules, indicating lack of coordination between Mg^{2+} and 4-nitrophenolate (**Figure 3.5b**). From these single-crystal studies, we observe that Ca^{2+} and Mg^{2+} ions interact with the 4-nitrophenolate molecule in distinctly different ways, in accordance with what is seen in the literature.[47,48]

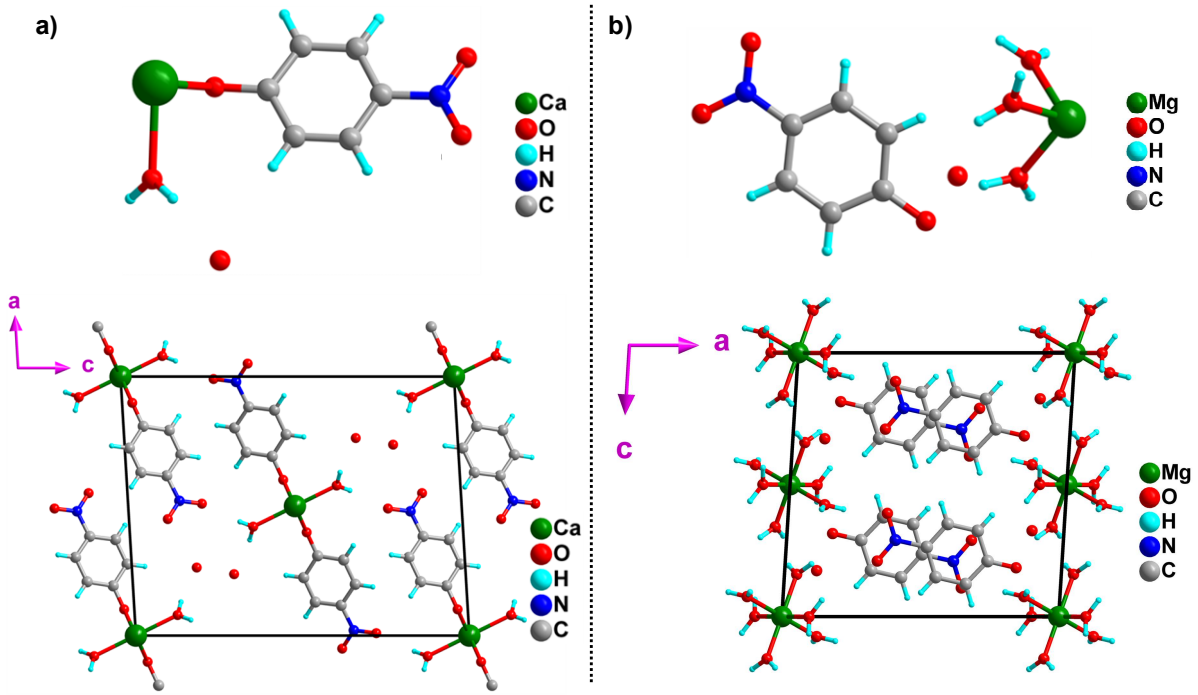

Figure 3.5. Crystallographic studies: a) Asymmetric unit (top) showing the interaction between Ca^{2+} ions (shown with green balls), and 4-nitrophenol molecule. Bottom panel shows the projection view of calcium 4-nitrophenolate crystal along the b axis, indicating the presence of coordination between the two. b) Asymmetric unit (top) showing the lack of interaction between Mg^{2+} ions (shown in green) and 4-nitrophenolate molecule. The bottom half of b) shows the projection of magnesium 4-nitrophenolate crystal along b-axis, indicating the lack of coordination between the two.

From these crystal structures, we can see that Ca^{2+} ions could interact and bridge between four 4-nitrophenolate molecules, while Mg^{2+} ions do not. This presence of additional bridging interactions in the case of Ca^{2+} ions could increase the amount of 4-nitrophenol molecules around the AuNPs, resulting in the higher local concentration of PNP. The presence of this additional bridging factor could assist the reduction of PNP, resulting in faster catalysis, when compared to Mg^{2+} ions.

3.6. Catalytic Reduction of Nitrobenzene

Secondly, [+] AuNP mediated reduction of nitrobenzene (NB) by $NaBH_4$ was performed in the presence of Ca^{2+} and Mg^{2+}, so as to investigate the influence of

specific-ion effects (see **Scheme 3.6.1.**). Here, the absence of the alcohol group in NB eliminates the possibility of coordination with Ca^{2+}, in accordance with the crystallographic study (see **Section 3.5.**).

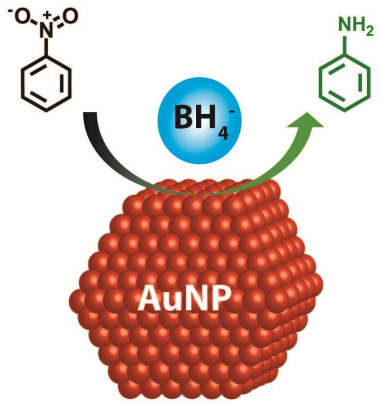

Scheme 3.6.1. Schematic representation of [+] AuNP catalyzed reduction of nitrobenzene (NB) to aniline by BH_4^- ions.

Here again, we used similar reaction conditions as were used for the reduction of PNP molecule. The main difference was that the stock solution of NB was made in methanol (**Figure 3.6a**). However the reduction reaction was carried out in milliQ water. In a typical experiment, 10 mM Ca^{2+} was added to a 10 mM solution of $NaBH_4$, followed by the addition of 20 pM of [+] AuNPs and 100 μM NB (for more details on experimental conditions, see **Section 2.4b**). The reaction was then monitored using UV-Vis. absorption spectroscopy at room temperature for ~2 h (see **Figure 3.6.**). **Figure 3.6b** shows the time-dependent variations in the absorption profiles of [+] AuNP mediated reduction of NB by BH_4^-. Here, the reduction process was accompanied by an increase in absorption intensity, as well as a bathochromic shift of ~13 nm, indicating the formation of N-phenylhydroxylamine intermediate.[43,44]This increase ceased after ~20 min, followed by a steady decrease in the absorption intensity at ~280 nm and a concomitant increase in the absorption intensity of aniline (product) at ~230 nm (see **Figure 3.6b**). Note that similar bathochromic shift and increase in the absorption intensity were observed in the presence of metal ions as well (see red and blue curves in **Figures 3.6c, d**). Rate constants for the reduction process were monitored by following the time-dependent absorption experiments at 279 nm in the presence, and absence of metal ions (see **Figures 3.6c,d**). Here again, we observed ~2 and ~3 times increment in the reaction rates, when Ca^{2+} and Mg^{2+} were added to the

reaction mixture (see **Figure 3.6d**). It should be noted that Mg^{2+} surpasses Ca^{2+} in accelerating the reduction of NB, a trend that is in accordance with variations in the strengths of the reducing agents.

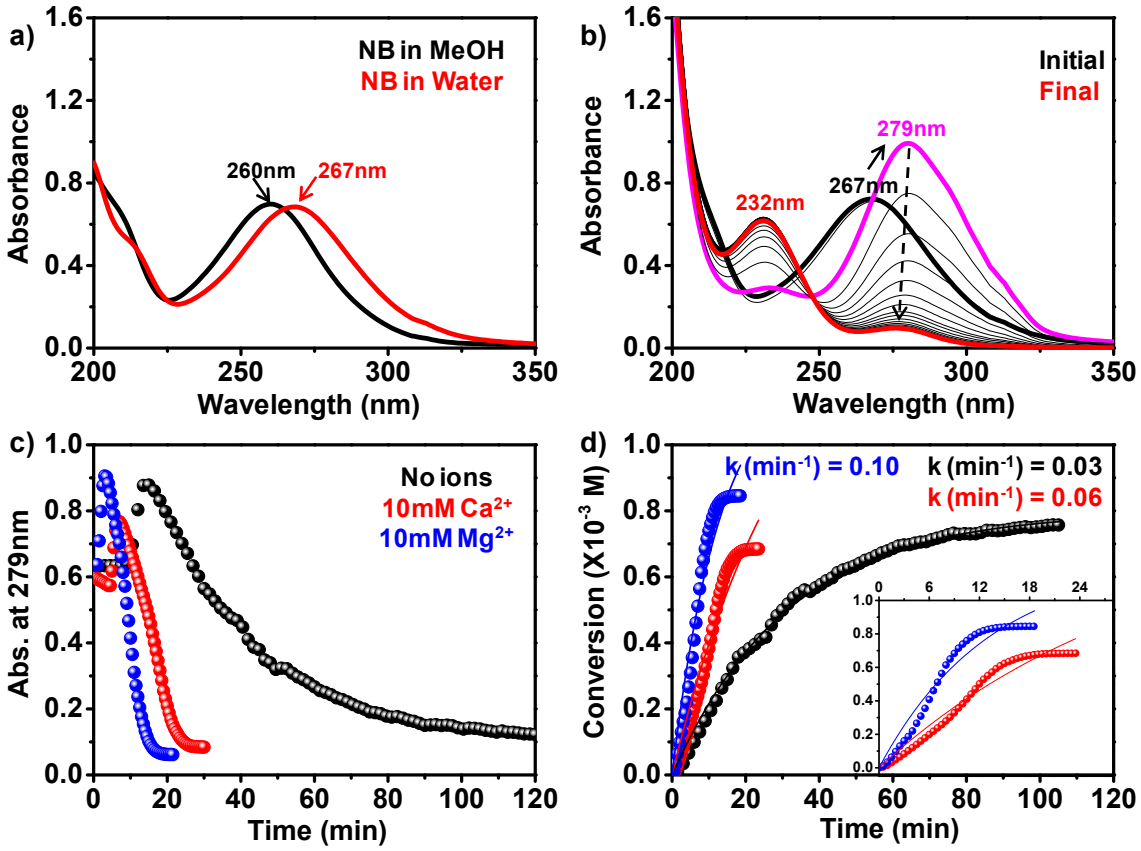

Figure 3.6. [+] AuNP catalyzed reduction of nitrobenzene (NB) by BH_4^- ions: a) UV-Vis. absorption spectra of NB (100 μM) in methanol and water, b) Variations in the UV-Vis. absorption spectra during the reduction of NB by BH_4^- in the presence of 0.1 mol % [+] AuNPs, c) Time-dependent absorption spectra at 279 nm, and d) corresponding first-order kinetic analysis in the presence and absence of metal ions.

Here, Mg^{2+}, being a stronger lewis acid than Ca^{2+}, results in the formation of stronger borohydride salt, and ultimately, faster reduction of NB. Both these studies (**Sections 3.5.** and **3.6.**) collectively reiterate the potent role of additional *specific-ion* effects in dictating the AuNP catalyzed PNP reduction by BH_4^- ions. This serendipitous result shows that '*stronger is not necessarily always better*'!

3.7. Ionic Strength Dependent Catalytic Reduction of PNP

The observed behaviour of accelerated reaction rates, in the presence of appropriate metal ions, is a counterintuitive finding. It has been already shown that, electrostatics

strongly dictates the outcomes of PNP reduction, and addition of salts to the solution results in screening of charges, and ultimately retarding the reaction (see **Figure 3.7a**).[11,49–51]To illustrate this point, we performed PNP reduction by BH_4^- with 20 pM [+] AuNPs, in 1X PBS, and 2X PBS. Addition of PBS resulted in the screening of charges and ultimately, a deceleration in the rate of reduction.

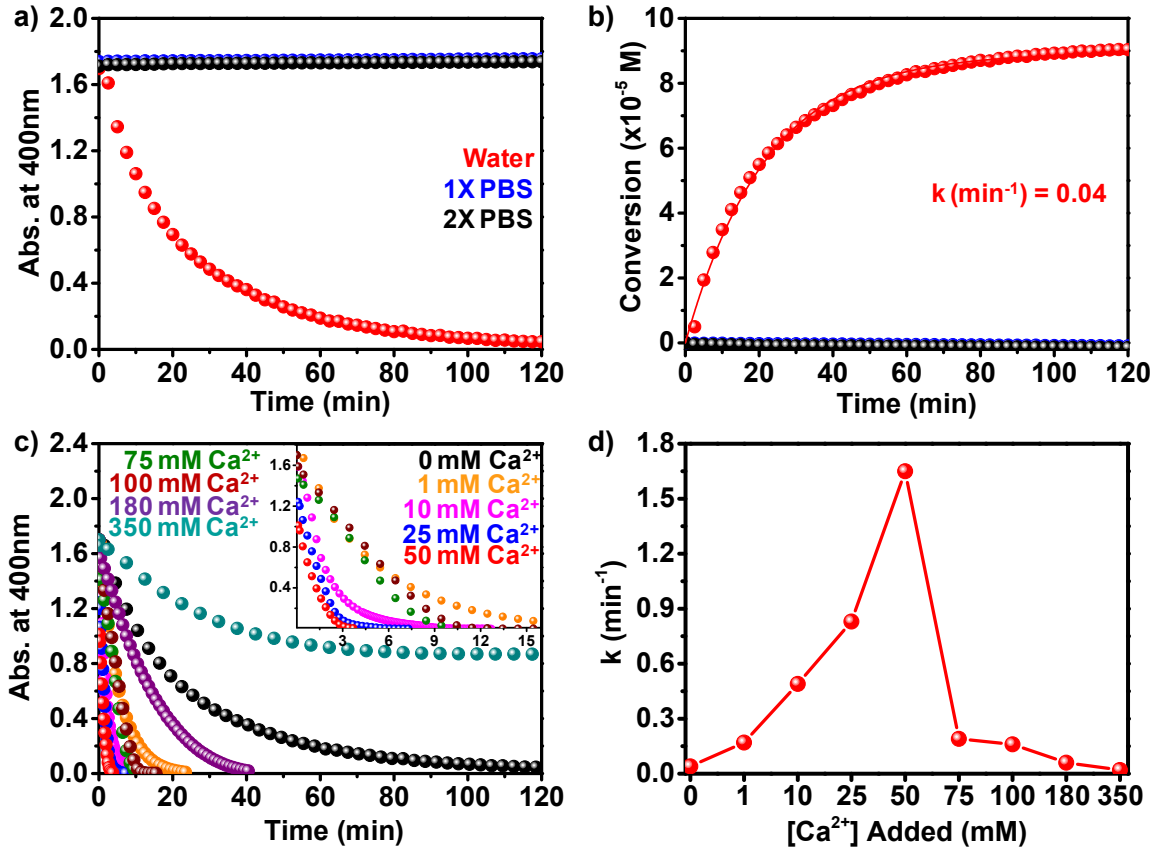

Figure 3.7. Deconvoluting ionic strength, and *specific-ion* effects in [+] AuNP catalyzed reduction of PNP by BH_4^- ions: a) Progress of PNP reduction in media of higher ionic strengths (i.e. 1X, and 2X PBS), and b) corresponding first-order kinetic analysis. c) Plot showing the progress of reaction in varying concentrations of Ca^{2+} ions (inset shows a zoomed graph, for the sake of better clarity), and d) variation in the rate constant as a function of the concentration of Ca^{2+} ions. Note that all these experiments were carried out in the presence of 10 mM BH_4^- ions and 0.1 mol % [+] AuNPs.

More precisely, we observed no noticeable catalysis of PNP by 0.1 mol % [+] AuNPs in the presence of both 1X, and 2X PBS (see **Figures 3.7a** and **b**). With this in mind, the present results demonstrating the acceleration of reaction rates in the presence of Ca^{2+} ions (see **Section 3.2.** to **Section 3.6.**) appear to be counterintuitive. In order to rationalize, and align the present finding with the conventional literature

knowledge, we performed a series of PNP reduction reactions in the presence of increasing concentrations of Ca^{2+} ions (from 1 mM to 350 mM). The results of these experiments are summarized in **Figures 3.7c** and **d**. We observed a systematic increase in reaction rates until a critical concentration of 50 mM of Ca^{2+} **(Figure 3.7d**). Further increments in Ca^{2+} ions resulted in a deceleration of the reaction rate, with catalysis completely ceasing in the presence of 350 mM Ca^{2+} ions (corresponding to the concentration of ions in 2X PBS). The present study, therefore, reveals an unexplored concentration regime, where combined effects of reducing power and coordination ability can overcome the ionic strength effects, resulting in improved catalytic conditions.

Next, in order to investigate the generality of the present findings, we performed similar PNP reduction reactions in the presence of appropriate metal ions with AuNPs having varying surface chemistries.

3.8. The Versatility of Our Idea: Studies with $[+/-]_4$ and [-] AuNPs

3.8.1. Synthesis and Characterization of $[+/-]_4$ and [-] AuNPs

To study the generality of the present findings, we thought of performing similar reduction reactions in the presence of AuNP catalysts with varying surface chemistries. We synthesized AuNPs with varying surface chemistries by using 11-mercaptoundecanoic acid (MUA, [-]) ligands to obtain negatively charged AuNPs ([-] AuNPs). Furthermore, we synthesized heterogeneously charged AuNPs by utilizing a mixture of [+], and [-] ligands during the place exchange protocol (see **Figure 3.8.1a**). The as-prepared AuNPs were well characterized using both UV-Vis. absorption and zeta potential studies. Here, we observed the zeta potential value increased from -38.1 ± 0.9 mV to -31.8 ± 1.0 mV when ~20 % of [-] charges were substituted with [+] ligands (see **Figures 3.8.1b** and **c**). With the desired AuNPs in our hands, we used them to catalyze PNP reduction reaction, to check the generality and flexibility of our idea.

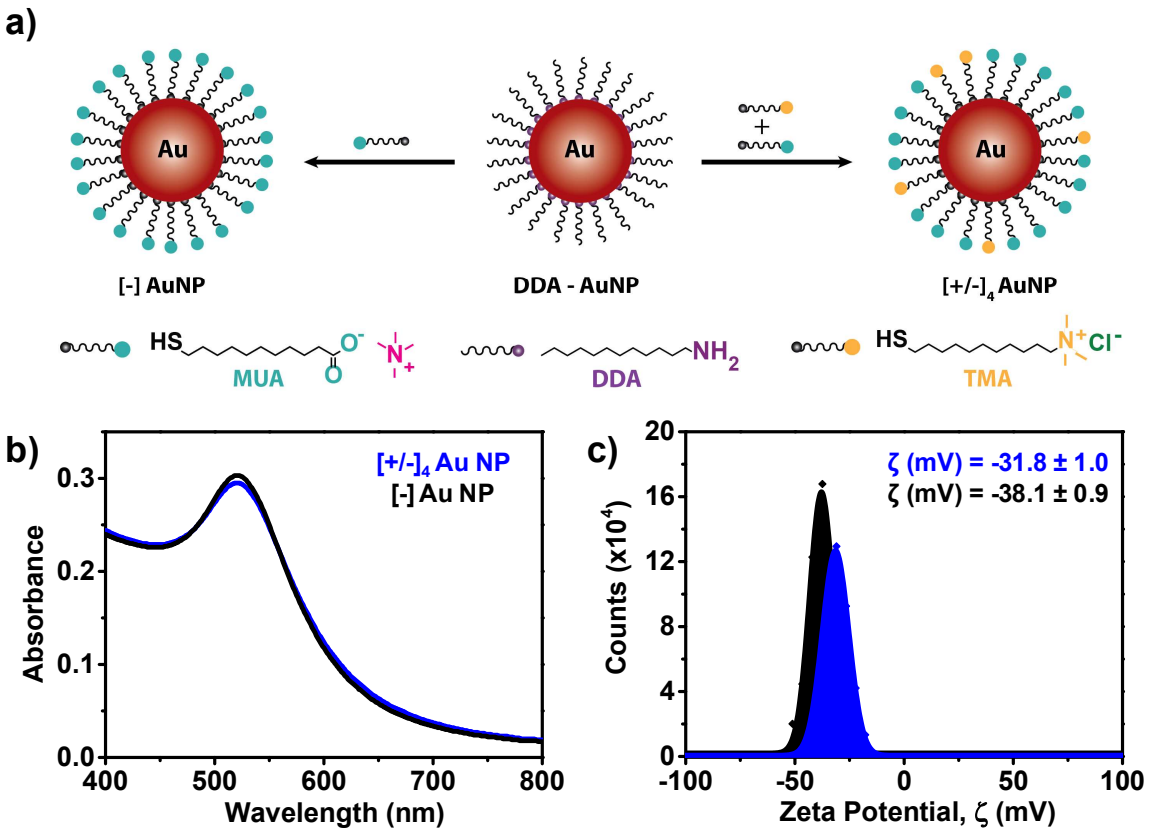

Figure 3.8.1. Synthesis and characterization of $[+/-]_4$ and [-] AuNPs: a) Schematics showing place exchange of DDA-AuNPs to obtain $[+/-]_4$ and [-] AuNPs. b) UV-Vis. absorption of $[+/-]_4$ (blue spectrum) and [-] (black spectrum), and c) a typical zeta potential plot of [-] and $[+/-]_4$ AuNPs.

3.8.2. PNP Reduction with $[+/-]_4$ AuNPs

Here again, we used similar reaction conditions as were used for the reduction of PNP molecule. In a typical experiment, 10 mM Ca^{2+} was added to a 10 mM solution of $NaBH_4$, followed by the addition of 20 pM of $[+/-]_4$ AuNPs and 100 μM PNP (for more details on experimental conditions, see **Section 2.4a**). **Figure 3.8.2.** shows the absorption changes at 400 nm for ~2 h in the presence and absence of different metal ions.

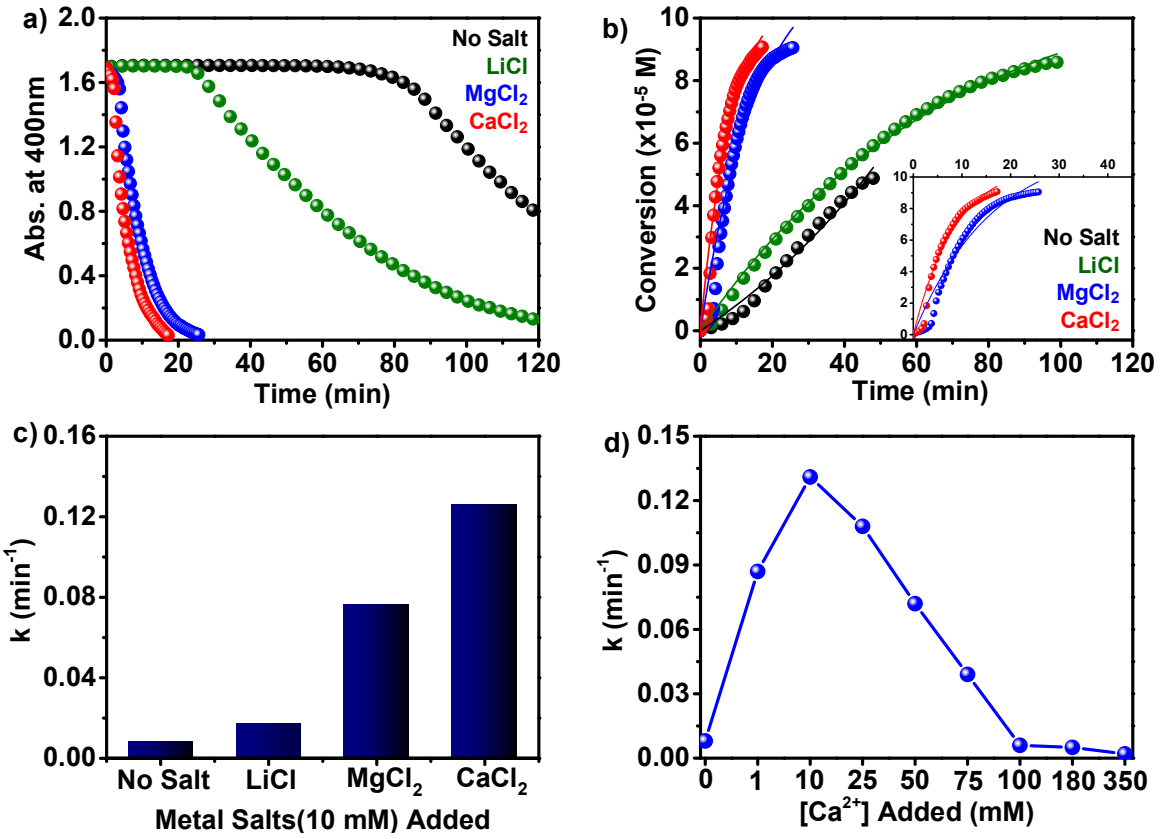

Figure 3.8.2. [+/-]$_4$ AuNP catalyzed reduction of PNP by BH_4^- ions: a) Reduction of PNP by BH_4^- ions (10 mM) using 0.1 mol % [+/-]$_4$ AuNPs in the presence of different metal salts, and b) the corresponding first-order kinetic analysis. c) Bar diagram showing the variation in the rate constant with respect to the nature of metal ions added to the solution. d) Plot summarizing variations in the rate constant of the PNP reduction reaction with varying concentrations of Ca^{2+} ions.

The presence of negative charges on the surface of NPs reduces the favourable electrostatic attractions with the negatively charged reactants, resulting in a decrease in reaction rate, when compared to [+] AuNPs (see **Figures 3.8.2a** and **b**). The rate constant of PNP reduction with [+/-]$_4$ AuNPs was ~5 times lower than what was observed for [+] AuNPs, along with an induction time of ~70 min (black curve in **Figures 3.8.2a** and **b**). Furthermore, we performed similar reduction reactions in the presence of different metal ions (10 mM of Li^+, Ca^{2+}, and Mg^{2+}) to study their influence on the catalytic performance of [+/-]$_4$ AuNPs (see **Figures 3.8.2a, b,** and **c**). Here again, we observed that the addition of Li^+, Ca^{2+}, and Mg^{2+} resulted in increments in reaction rates, as was observed with [+] AuNPs (see **Section 3.3**). These results are summarized in **Table 3.8.1.** Interestingly, we observed that with [+/-]$_4$ AuNPs as well, Ca^{2+} ions outperformed Mg^{2+} ions despite being a comparatively weaker reducing agent. Here again, we performed concentration-

dependent studies with Ca^{2+} ions to reveal and deconvolute accelerated reaction rate regime from ionic strength effects (see **Figure 3.8.2d**). We observed a systematic, and consistent increase in the rate constant values till 10 mM, while further increase in the concentration of Ca^{2+} ions resulted in a steady decrease in reaction rate. It should be noted that the reaction ceased at 100-150 mM of Ca^{2+} ions. These results, again demonstrate the unexplored regime where, the addition of metal ions can result in an increase in the reaction rates, and dominate ionic strength effects at higher concentration values.

S.No.	Metal Salt Added (10 mM)	Induction Time (min)	k (min^{-1})
1	No Salt	73.4	0.008
2	LiCl	22.4	0.017
3	$MgCl_2$	2.2	0.076
4	$CaCl_2$	0.7	0.126

Table 3.8.1. Table summarizing the effect of different metal ions on the rate constant, as well as induction time in 0.1 mol % $[+/-]_4$ AuNP catalyzed reduction of PNP by BH_4^- ions.

3.9. Converting Non-Catalytic Systems to Catalytic Systems

The idea of '*introducing metal salts*' to influence and improve AuNP catalyzed PNP reduction can have significant impacts in future catalytic chemical transformations. With this in mind, we show that the knowledge gained can be exploited to convert a non-catalytic system to a catalytically active one (see **Figure 3.9.**). In this direction, we show two studies, where,

a) the concentration of [+] AuNPs was dropped from 20 pM to 5 pM (see **Figures 3.9a, b**), and

b) convert a non-catalytic system of [-] AuNPs[11]to a catalytically active one (see **Figures 3.9c, d**).

We note that 5 pM of [+] AuNPs failed to catalyze the conversion of PNP to PAP even after ~4 h (see black curve in **Figure 3.9a**). The addition of 10 mM Mg^{2+}ions to the reaction mixture improved the catalytic activity. After an induction time of ~40 min, all of the PNP reduced to PAP in ~4 h with a rate constant of 0.01 min^{-1} (see

blue curve in **Figures 3.9a, b**). Interestingly, the addition of 10 mM Ca^{2+} ions enhanced the rate constant of the reduction reaction. All of the PNP was converted to PAP within ~2 h, with a rate constant of 0.02 min^{-1} (see red curve in **Figures 3.9a, b**). These experiments show that by optimizing the reaction conditions, we can decrease the catalyst amounts from ~20 pM (0.1 mol %) to ~5 pM (0.03 mol %). Furthermore, we could convert a catalytically inactive system ([-] AuNPs)[11] to a catalytically active one in the presence of Ca^{2+} ions. Here, we note that 20 pM of [-] AuNPs failed to reduce PNP, even after ~2 days (see black curve in **Figures 3.9c, d**), whereas the presence of 10 mM Ca^{2+} or 10 mM Mg^{2+} ions in the reaction medium can conveniently reduce all the PNP to PAP within 20, or 30 min respectively (see **Figures 3.9c** and **d**).

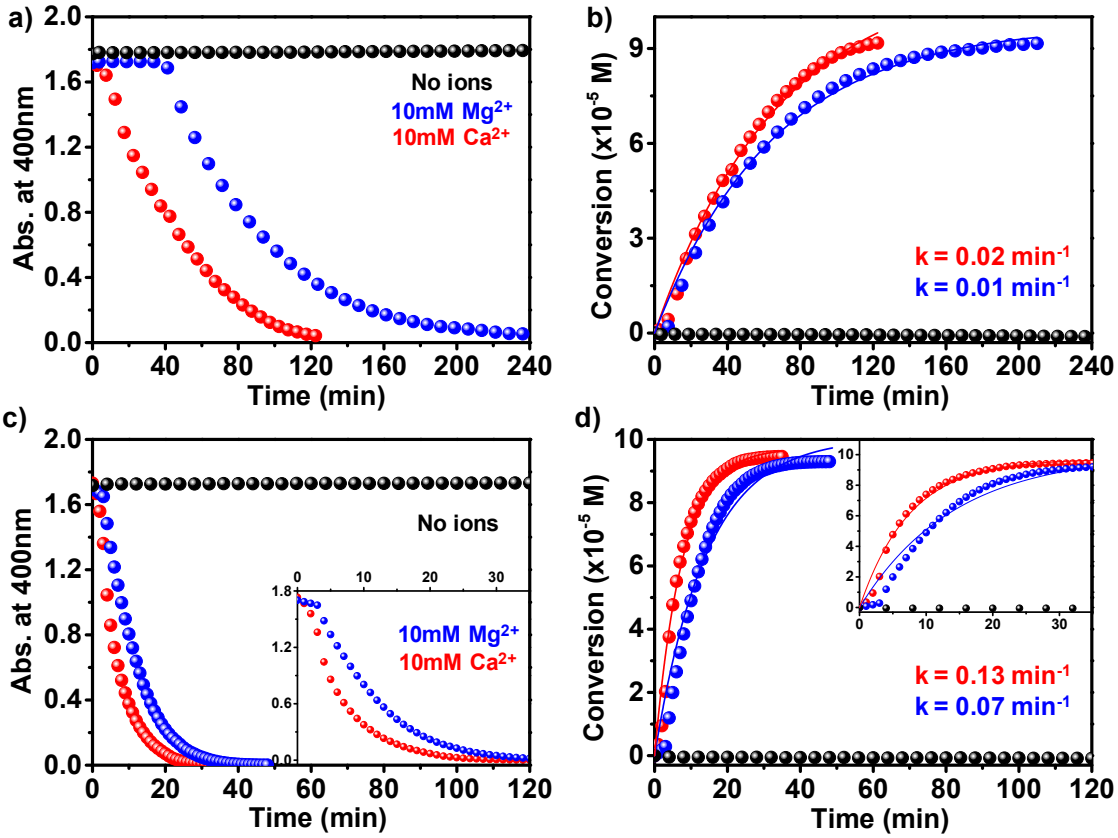

Figure 3.9. Conversion of non- catalytic systems to catalytically active ones: a) Plot showing the conversion of a non-catalytic system (0.03 mol % [+] AuNPs; shown in black) into a catalytically active one in the presence of Ca^{2+} (shown in red), and Mg^{2+} ions (shown in blue). b) Estimation of the rate constants from first-order kinetic analysis. c) and d) shows conversion of another non-catalytic system (0.1 mol % [-] AuNPs) to catalytically active one in the presence of Ca^{2+} and Mg^{2+} ions.

4

Conclusions

The present study revealed the prodigious effects of reaction conditions on AuNP catalyzed PNP reduction reactions. Here, we carry out a thorough investigation, where AuNP catalyzed reduction of PNP by $NaBH_4$ was carried out in the presence of various metal ions (resulting in formation of stronger reducing agents). In principle, introduction of stronger reducing agents should monotonically enhance the performance of any reduction reaction. We, however, demonstrate that reducing ability of borohydride ions is an incomplete descriptor to explain the variations observed with the addition of different metal ions. We note that increments in the reduction rates clearly followed the reducing strength of borohydrides in case of monovalent cations. Surprisingly, in the case of divalent ions, the addition of Ca^{2+} ions in reaction mixture improved the PNP reduction rate by ~12 times compared to Mg^{2+} ions (~7 times), despite $Ca(BH_4)_2$ being a weaker reducing agent than $Mg(BH_4)_2$. This serendipitous observation is rationalized to be originating because of *specific-ion* effects, in addition to the reducing ability of borohydride. Control experiments (like crystallographic studies and NB reduction) demonstrate the necessity of bridging interactions in enhancing the reduction rate with Ca^{2+}, over Mg^{2+} ions. The bridging between Ca^{2+} and 4-nitrophenolate ions increases the channelling and local concentration of reactants around the AuNP catalyst, thereby enhancing the rate of the reaction. The present results, therefore, show that '*stronger reducing agent is not necessarily better*' for AuNP catalyzed PNP reduction by BH_4^- ions. The potency of metal assisted enhancement in the reaction rates was then exploited to reduce the catalyst amounts from 20 pM to 5 pM, and convert a non-catalytic system into catalytically active one.

Thus, our study shows that how simple variations in the reaction conditions can have significant impacts in the field of chemical transformations.

References

(1) Christopher, P.; Xin, H.; Linic, S. Visible-Light-Enhanced Catalytic Oxidation Reactions on Plasmonic Silver Nanostructures. *Nat. Chem.,* **2011**, *3*, 467–472.

(2) Kim, Y.; Dumett Torres, D.; Jain, P. K. Activation Energies of Plasmonic Catalysts. *Nano Lett.,* **2016**, *16*, 3399–3407.

(3) Narayanan, R.; El-Sayed, M. A. Catalysis with Transition Metal Nanoparticles in Colloidal Solution: Nanoparticle Shape Dependence and Stability. *J. Phys. Chem. B,* **2005**, *109*, 12663–12676.

(4) Linic, S.; Christopher, P.; Xin, H.; Marimuthu, A. Catalytic and Photocatalytic Transformations on Metal Nanoparticles with Targeted Geometric and Plasmonic Properties. *Acc. Chem. Res.,* **2013**, *46*, 1890–1899.

(5) Lopez, N.; Nørskov, J. K. Catalytic CO Oxidation by a Gold Nanoparticle: A Density Functional Study. *J. Am. Chem. Soc.,* **2002**, *124*, 11262–11263.

(6) Kale, M. J.; Avanesian, T.; Christopher, P. Direct Photocatalysis by Plasmonic Nanostructures. *ACS Catal.,* **2014**, *4*, 116–128.

(7) Astruc, D.; Lu, F.; Aranzaes, J. R. Nanoparticles as Recyclable Catalysts: The Frontier between Homogeneous and Heterogeneous Catalysis. *Angew. Chem. Int. Ed.,* **2005**, *44*, 7852–7872.

(8) Turner, M.; Golovko, V. B.; Vaughan, O. P. H.; Abdulkin, P.; Berenguer-Murcia, A.; Tikhov, M. S.; Johnson, B. F. G.; Lambert, R. M. Selective Oxidation with Dioxygen by Gold Nanoparticle Catalysts Derived from 55-Atom Clusters. *Nature,* **2008**, *454*, 981–983.

(9) Pradhan, N.; Pal, A.; Pal, T. Silver Nanoparticle Catalyzed Reduction of Aromatic Nitro Compounds. *Colloids Surf. A,* **2002**, *196*, 247–257.

(10) Zhou, D.; Li, Y. C.; Xu, P.; McCool, N. S.; Li, L.; Wang, W.; Mallouk, T. E. Visible-Light Controlled Catalytic Cu2O–Au Micromotors. *Nanoscale,* **2016**, *9*, 75–78.

(11) Roy, S.; Rao, A.; Devatha, G.; Pillai, P. P. Revealing the Role of Electrostatics in Gold-Nanoparticle-Catalyzed Reduction of Charged Substrates. *ACS Catal.,* **2017**, *7*, 7141–7145.

(12) Li, M.; Chen, G. Revisiting Catalytic Model Reaction p -Nitrophenol/NaBH 4 Using Metallic Nanoparticles Coated on Polymeric Spheres. *Nanoscale,* **2013**, *5*, 11919–11927.

(13) Hervés, P.; Pérez-Lorenzo, M.; Liz-Marzán, L. M.; Dzubiella, J.; Lu, Y.; Ballauff, M. Catalysis by Metallic Nanoparticles in Aqueous Solution: Model Reactions. *Chem. Soc. Rev.,* **2012**, *41*, 5577–5587.

(14) Huang, C.; Ye, W.; Liu, Q.; Qiu, X. Dispersed Cu2O Octahedrons on H-BN Nanosheets for p-Nitrophenol Reduction. *ACS Appl. Mater. Interfaces,* **2014**, *6*, 14469–14476.

(15) Liang, Y.; Manioudakis, J.; Macairan, J.-R.; Askari, M. S.; Forgione, P.; Naccache, R. Facile Aqueous-Phase Synthesis of an Ultrasmall Bismuth Nanocatalyst for the Reduction of 4-Nitrophenol. *ACS Omega,* **2019**, *4*, 14955–14961.

(16) Kong, X.; Sun, Z.; Chen, M.; Chen, C.; Chen, Q. Metal-Free Catalytic Reduction of 4-Nitrophenol to 4-Aminophenol by N-Doped Graphene. *Energy Environ. Sci.,* **2013**, *6*, 3260–3266.

(17) Jin, L.; Zhao, X.; Ye, J.; Qian, X.; Dong, M. MOF-Derived Magnetic Ni-Carbon Submicrorods for the Catalytic Reduction of 4-Nitrophenol. *Catal. Commun.,***2018**, *107*, 43–47.

(18) Sadeghzadeh, S. M.; Zhiani, R.; Emrani, S. The Reduction of 4-Nitrophenol and 2-Nitroaniline by the Incorporation of Ni@Pd MNPs into Modified UiO-66-NH2 Metal–Organic Frameworks (MOFs) with Tetrathia-Azacyclopentadecane. *New J. Chem.,* **2018**, *42*, 988–994.

(19) Liu, J.; Yan, X.; Wang, L.; Kong, L.; Jian, P. Three-Dimensional Nitrogen-Doped Graphene Foam as Metal-Free Catalyst for the Hydrogenation Reduction of p-Nitrophenol. *J. Colloid Interf. Sci.,* **2017**, *497*, 102–107.

(20) Sahiner, N.; Sagbas, S.; Aktas, N. Very Fast Catalytic Reduction of 4-Nitrophenol, Methylene Blue and Eosin Y in Natural Waters Using Green Chemistry: P(Tannic Acid)–Cu Ionic Liquid Composites. *RSC Adv.,* **2015**, *5*, 18183–18195.

(21) Wunder, S.; Lu, Y.; Albrecht, M.; Ballauff, M. Catalytic Activity of Faceted Gold Nanoparticles Studied by a Model Reaction: Evidence for Substrate-Induced Surface Restructuring. *ACS Catal.,* **2011**, *1*, 908–916.

(22) Pradhan, N.; Pal, A.; Pal, T. Catalytic Reduction of Aromatic Nitro Compounds by Coinage Metal Nanoparticles. *Langmuir,* **2001**, *17*, 1800–1802.

(23) Ansar, S. M.; Kitchens, C. L. Impact of Gold Nanoparticle Stabilizing Ligands on the Colloidal Catalytic Reduction of 4-Nitrophenol. *ACS Catal.,* **2016**, *6*, 5553–5560.

(24) Ciganda, R.; Li, N.; Deraedt, C.; Gatard, S.; Zhao, P.; Salmon, L.; Hernández, R.; Ruiz, J.; Astruc, D. Gold Nanoparticles as Electron Reservoir Redox Catalysts for 4-Nitrophenol Reduction: A Strong Stereoelectronic Ligand Influence. *Chem. Commun.,* **2014**, *50*, 10126–10129.

(25) Wei, J.; Wang, H.; Deng, Y.; Sun, Z.; Shi, L.; Tu, B.; Luqman, M.; Zhao, D. Solvent Evaporation Induced Aggregating Assembly Approach to Three-Dimensional Ordered Mesoporous Silica with Ultralarge Accessible Mesopores. *J. Am. Chem. Soc.,* **2011**, *133*, 20369–20377.

(26) Zhou, X.; Xu, W.; Liu, G.; Panda, D.; Chen, P. Size-Dependent Catalytic Activity and Dynamics of Gold Nanoparticles at the Single-Molecule Level. *J. Am. Chem. Soc.,* **2010**, *132*, 138–146.

(27) Mahmoud, M. A.; Saira, F.; El-Sayed, M. A. Experimental Evidence For The Nanocage Effect In Catalysis With Hollow Nanoparticles. *Nano Lett.,* **2010**, *10*, 3764–3769.

(28) Zeng, J.; Zhang, Q.; Chen, J.; Xia, Y. A Comparison Study of the Catalytic Properties of Au-Based Nanocages, Nanoboxes, and Nanoparticles. *Nano Lett.,* **2010**, *10*, 30–35.

(29) Ghosh, S. K.; Kundu, S.; Mandal, M.; Pal, T. Silver and Gold Nanocluster Catalyzed Reduction of Methylene Blue by Arsine in a Micellar Medium. *Langmuir,* **2002**, *18*, 8756–8760.

(30) Cleve, T. V.; Moniri, S.; Belok, G.; More, K. L.; Linic, S. Nanoscale Engineering of Efficient Oxygen Reduction Electrocatalysts by Tailoring the Local Chemical Environment of Pt Surface Sites. *ACS Catal.,* **2017**, *7*, 17–24.

(31) Kim, J.-H.; Lavin, B. W.; Boote, B. W.; Pham, J. A. Photothermally Enhanced Catalytic Activity of Partially Aggregated Gold Nanoparticles. *J Nanopart Res,* **2012**, *14*, 995.

(32) Menumerov, E.; Hughes, R. A.; Neretina, S. Catalytic Reduction of 4-Nitrophenol: A Quantitative Assessment of the Role of Dissolved Oxygen in Determining the Induction Time. *Nano Lett.,* **2016**, *16*, 7791–7797.

(33) Choi, S.; Jeong, Y.; Yu, J. Spontaneous Hydrolysis of Borohydride Required before Its Catalytic Activation by Metal Nanoparticles. *Catal.Commun.,***2016**, *84*, 80–84.

(34) Carey, F. A.; Sundberg, R. J. *Advanced Organic Chemistry: Part A: Structure and Mechanisms*; Springer Science & Business Media, **2007**.

(35) Carey, F. A.; Sundberg, R. J. *Advanced Organic Chemistry: Part B: Reaction and Synthesis*; Springer Science & Business Media, **2007**.

(36) Brown, H. C.; Rao, B. C. S. A New Powerful Reducing Agent—Sodium Borohydride in the Presence of Aluminum Chloride and Other Polyvalent Metal Halides1,2. *J. Am. Chem. Soc.,* **1956**, *78*, 2582–2588.

(37) Tien, J.; Terfort, A.; Whitesides, G. M. Microfabrication through Electrostatic Self-Assembly. *Langmuir,* **1997**, *13*, 5349–5355.

(38) Jana, N. R.; Peng, X. Single-Phase and Gram-Scale Routes toward Nearly Monodisperse Au and Other Noble Metal Nanocrystals. *J. Am. Chem. Soc.,* **2003**, *125*, 14280–14281.

(39) Pillai, P. P.; Huda, S.; Kowalczyk, B.; Grzybowski, B. A. Controlled pH Stability and Adjustable Cellular Uptake of Mixed-Charge Nanoparticles. *J. Am. Chem. Soc.,* **2013**, *135*, 6392–6395.

(40) Rao, A.; Roy, S.; Unnikrishnan, M.; Bhosale, S. S.; Devatha, G.; Pillai, P. P. Regulation of Interparticle Forces Reveals Controlled Aggregation in Charged Nanoparticles. *Chem. Mater.,* **2016**, *28*, 2348–2355.

(41) Liu, X.; Atwater, M.; Wang, J.; Huo, Q. Extinction Coefficient of Gold Nanoparticles with Different Sizes and Different Capping Ligands. *Colloids Surf. B,* **2007**, *58*, 3–7.

(42) Van Etten, R. L.; McTigue, J. J.; pH dependence and solvent isotope effects in the hydrolysis of phosphomonoesters by human prostatic acid phosphatase. *Biochim. Biophys. Acta,* **1977**, *484,* 386–397.

(43) Doherty, S.; Knight, J. G.; Backhouse, T.; Summers, R. J.; Abood, E.; Simpson, W.; Paget, W.; Bourne, R. A.; Chamberlain, T. W.; Stones, R.; Lovelock, K. R. J.; Seymour, J. M.; Isaacs, M. A.; Hardacre, C.; Daly, H.; Rees, N. H. Highly Selective and Solvent-Dependent Reduction of Nitrobenzene to

N-Phenylhydroxylamine, Azoxybenzene, and Aniline Catalyzed by Phosphino-Modified Polymer Immobilized Ionic Liquid-Stabilized AuNPs. *ACS Catal.,***2019**, *9*, 4777–4791.

(44) Liu, A.; Traulsen, C. H.-H.; Cornelissen, J. J. L. M.; Nitroarene Reduction by a Virus Protein Cage Based Nanoreactor. *ACS Catal.,* **2016**, *6*, 3084–3091.

(45) Weast, R. C.; *Handbook of Chemistry and Physics*; CRC Press Inc., **1979**.

(46) Hawthorne, F. C.; A bond-topological approach to theoretical mineralogy: crystal structure, chemical composition and chemical reactions. *Phys Chem Minerals,* **2012**, *39*, 841–874.

(47) Muthuraman, M.; Bagieu-Beucher, M.; Masse, R.; Nicoud, J.-F.; Desiraju, G. R. Sodium 4-Nitrophenolate 4-Nitrophenol Dihydrate Crystal: A New Herringbone Structure for Quadratic Nonlinear Optics. *J. Mat. Chem.,* **1999**, *9*, 1471–1479.

(48) Brent Cole, L.; M. Holt, E. Structural Comparison of Calcium and Magnesium Binding to 2,4-Dinitrophenoxide. *J. Chem. Soc., Perkin Trans. 2,* **1986**, *0*, 1997–2002.

(49) Devatha, G.; Roy, S.; Rao, A.; Mallick, A.; Basu, S.; Pillai, P. P. Electrostatically Driven Resonance Energy Transfer in “Cationic” Biocompatible Indium Phosphide Quantum Dots. *Chem. Sci.,* **2017**, *8*, 3879–3884.

(50) Bishop, K. J. M.; Wilmer, C. E.; Soh, S.; Grzybowski, B. A. Nanoscale Forces and Their Uses in Self-Assembly. *Small,* **2009**, *5*, 1600–1630.

(51) Bishop, K. J. M.; Kowalczyk, B.; Grzybowski, B. A. Precipitation of Oppositely Charged Nanoparticles by Dilution and/or Temperature Increase. *J. Phys. Chem. B,* **2009**, *113*, 1413–1417.

■